

1 **Gut Microbiome Pattern Reflects Healthy Aging and Predicts Extended Survival in**  
2 **Humans**

3 Tomasz Wilmanski<sup>1</sup>, Christian Diener<sup>1</sup>, Noa Rappaport<sup>1</sup>, Sushmita Patwardhan<sup>1</sup>, Jack Wiedrick<sup>2</sup>,  
4 Jodi Lapidus<sup>2</sup>, John C. Earls<sup>1</sup>, Anat Zimmer<sup>1</sup>, Gustavo Glusman<sup>1</sup>, Max Robinson<sup>1</sup>, James T.  
5 Turkovich<sup>1</sup>, Deborah M. Kado<sup>3</sup>, Jane A. Cauley<sup>4</sup>, Joseph Zmuda<sup>4</sup>, Nancy E. Lane<sup>5</sup>, Andrew T.  
6 Magis<sup>1</sup>, Jennifer C. Lovejoy<sup>1</sup>, Leroy Hood<sup>1</sup>, Sean M. Gibbons\*<sup>1,6,7</sup>, Eric S. Orwoll\*<sup>2</sup>, & Nathan  
7 Price\*<sup>1</sup>

8 **Affiliations:**

9 <sup>1</sup>Institute for Systems Biology, Seattle, WA 98109

10 <sup>2</sup>Oregon Health and Science University, Portland, OR 97239

11 <sup>3</sup>Departments of Family Medicine and Public Health and Internal Medicine, University of  
12 California San Diego, La Jolla, CA 92093

13 <sup>4</sup>Department of Epidemiology, University of Pittsburgh, Pittsburgh, PA 15261

14 <sup>5</sup>Center for Musculoskeletal Health, Department of Internal Medicine, University of California  
15 Davis Medical Center, Sacramento, CA 95817

16 <sup>6</sup>eScience Institute, University of Washington, Seattle, WA 98195

17 <sup>7</sup>Department of Bioengineering, University of Washington, Seattle, WA 98195

18 \*Correspondence to: [sgibbons@isbscience.org](mailto:sgibbons@isbscience.org), [orwoll@ohsu.edu](mailto:orwoll@ohsu.edu), [nprice@isbscience.org](mailto:nprice@isbscience.org).

19  
20 **Abstract:** The gut microbiome has important effects on human health, yet its importance in  
21 human aging remains unclear. Using two independent cohorts comprising 4582 individuals  
22 across the adult lifespan we demonstrate that, starting in mid-to-late adulthood, gut microbiomes  
23 become increasingly unique with age. This uniqueness pattern is strongly associated with gut  
24 microbial amino acid derivatives circulating within the bloodstream, many of which have been  
25 previously identified as longevity biomarkers. At the latest stages of human life, two distinct  
26 patterns emerge wherein individuals in good health show continued microbial drift toward a  
27 unique compositional state, while the same drift is absent in individuals who perform worse on a  
28 number of validated health measures. The identified healthy aging pattern is characterized by an  
29 overall depletion of core genera found across most humans - primarily a depletion in the nearly  
30 ubiquitous genus *Bacteroides*. Consistently, retaining a high *Bacteroides* dominance into  
31 extreme age, or, equivalently, having a low gut microbiome uniqueness score, predicts decreased  
32 survival in a four-year follow-up. Our comprehensive analysis identifies the gut microbiome as a  
33 novel component of healthy aging, with important implications for the world's growing older  
34 population.

44

## Introduction

45

The human gut harbors a diverse microbial ecosystem that has increasingly been shown to play an important role in host health<sup>1-3</sup>. Despite considerable progress in our understanding of the gut microbiome, very little is known about how it changes with age and how these changes interact with host physiology. Furthermore, there is no consensus on whether or not age-associated changes in the gut microbiome are related to the health state of the host. Importantly, identification of aging patterns within the gut microbiome could have major clinical implications for both monitoring and modifying gut microbiome health throughout life.

52

Several studies conducted on centenarian populations provided potential insight into gut microbial trajectories associated with aging. Biagi *et al.*<sup>4</sup> demonstrated that gut microbiomes of centenarians ( $\leq 104$  years of age) and supercentenarians (104+ years) show a depletion in core abundant taxa (*Bacteroides*, *Roseburia* and *Faecalibacterium*, among others), complemented by an increase in the prevalence of rare taxa. Similar findings have since been reported in other centenarian populations across the world, such as in Sardinian, Chinese and Korean centenarians, relative to healthy, younger controls<sup>5-7</sup>. Some studies have also reported higher  $\alpha$ -diversity in centenarians compared to younger individuals<sup>6-8</sup>, suggesting that the gut microbiome continues to develop within its host even in the latest decades of human life.

60

Gut microbial associations reported in centenarians often contradict findings reported in younger elderly populations. In particular, studies on the ELDERMET cohort (i.e. the most extensively studied cohort of older persons with gut microbiome data to date) reported an increased dominance of the core genera *Bacteroides*, *Alistipes* and *Parabacteroides* in those 65+ years old compared to healthy, younger controls<sup>9</sup>. Studies on older long-term care residents further demonstrated a gradual change in microbiome composition associated with duration of stay in the care facility, which has been attributed to changes in diet and lifestyle<sup>10,11</sup>. Collectively, these and other studies<sup>12,13</sup> provide a view of the human gut microbiome as relatively stable up until old age, at which point gradual compositional shifts occur that are driven by dietary and lifestyle changes, as well as declining health.

68

The often-contradictory findings in elderly and centenarian populations indicate there may exist multiple gut microbiome patterns of aging, some of which reflect better health and life expectancy outcomes than others. Although recent analyses have demonstrated a link between gut microbiome composition and long-term health outcomes<sup>3,14</sup>, the scarcity of elderly cohorts with longitudinal follow-up data, the lack of detailed molecular phenotyping and health metrics, and the relatively small sample sizes of existing studies on aging limit our understanding of gut microbial changes seen across the human lifespan. In the present study, we overcome these limitations and present an analysis of the gut microbiome and phenotypic data from 4582 individuals spanning 18 to 98 years of age, with longitudinal follow-up data in an older cohort that allowed us to track survival outcomes.

76

## Results

77

We studied two distinct cohorts: a deeply phenotyped population of individuals who self-enrolled in a scientific wellness company (the ‘Arivale cohort’, ages 18-87) (**Table S1**) and the Osteoporotic Fractures in Men (MrOS) cohort (ages 78-98)<sup>15-17</sup> (**Table S2**) (**Fig. 1**). These cohorts further subdivide into two groups each. The MrOS cohort separates into a discovery cohort (N=599) and a validation cohort (N=308), because stool samples from this population were processed in two separate batches several years apart. The Arivale cohort separates into Group A (N=2539) and Group B (N=1114), where the distinguishing factor is the use of

90 different vendors for the collection and processing of stool samples (see Methods). We began by  
91 analyzing baseline data from the Arivale cohort to identify gut microbial aging patterns across  
92 most of the adult human lifespan, and investigate how these patterns correspond to host  
93 physiology. We then extended our analysis to the MrOS cohort, where we had detailed health  
94 metrics and follow-up data on mortality, to evaluate how the patterns identified within the  
95 Arivale cohort correspond to health and survival in the latter decades of human life.  
96

### 97 ***A gut microbiome aging pattern that spans much of the adult lifespan***

98 To characterize gut microbial patterns associated with aging, we initially performed a  $\beta$ -diversity  
99 analysis comparing all available baseline microbiome samples from a heterogenous, and  
100 relatively healthy Arivale population (Fig. 1 and Table S1). Our analysis involved extracting the  
101 minimum value for each individual from a calculated Bray-Curtis dissimilarity matrix. This  
102 value reflects how dissimilar an individual is from their nearest neighbor, given all other gut  
103 microbiome samples in the cohort. We refer to this as a measure of ‘uniqueness’: the higher the  
104 value, the more distinct the gut microbiome is from everyone else’s in the studied population.  
105 Arivale participants showed initial drift toward an increasingly unique gut microbiome  
106 composition starting between 40-50 years of age, and this continued to increase with every  
107 passing decade (linear models adjusted for age, body mass index (BMI), sex and Shannon  
108 diversity) (Fig. 2A). We replicated our analysis using additional  $\beta$ -diversity metrics. Uniqueness  
109 based on Weighted UniFrac demonstrated a similar positive association with age across both  
110 vendors, while Jaccard and Unweighted UniFrac metrics resulted in either a weaker association  
111 (vendor B) or no association (vendor A) with age (Fig. 2B). These results indicate that the  
112 observed age-related increase in uniqueness is likely not a result of the loss or acquisition of  
113 microbial genera in older individuals, which would increase unweighted  $\beta$ -diversity and Jaccard  
114 distance measures, but rather is driven more by shifts in relative abundance of microbes already  
115 present in the ecosystem.

116 To further characterize the observed gut microbiome aging pattern, and understand how it  
117 is reflected in host physiology and health, we combined data from both Arivale vendors (Fig.  
118 2C) and tested the correspondence between Bray-Curtis uniqueness and a wide variety of clinical  
119 laboratory tests, demographic information, and self-reported lifestyle/health measures, adjusting  
120 for microbiome vendor (Fig. 2D, Table S3). Of all the factors tested, age demonstrated the  
121 strongest association with gut microbial uniqueness. Several other factors were significantly  
122 associated with uniqueness, but many of them were no longer significant after adjusting for age.  
123 In fact, after adjusting for age, essentially only lipid markers and BMI remained significantly  
124 associated with gut microbial uniqueness, with the direction of association indicating healthier  
125 metabolic and lipid profiles in individuals with more unique gut microbiomes: e.g. lower BMI,  
126 lower n6/n3 fatty acid ratio, higher high-density lipoprotein (HDL) cholesterol, lower low  
127 density lipoprotein (LDL) cholesterol, higher vitamin D, and lower triglycerides in individuals  
128 with more unique microbiomes (Fig. 2D). Interestingly, self-reported dietary measures showed  
129 no association with our gut microbiome uniqueness score, suggesting that the identified gut  
130 microbial aging pattern is not driven by self-reported differences in dietary habits.

131 Women have an extended average lifespan compared to men<sup>18</sup>, with previous studies  
132 also indicating varying aging patterns across sex<sup>19,20</sup>. To evaluate whether the observed  
133 increased uniqueness with age is sex-dependent, we investigated the association of age with  
134 Bray-Curtis uniqueness independently in men and women, adjusting for age, BMI, Shannon  
135 diversity and microbiome vendor. Although both sexes showed a significant positive association

136 between age and our gut microbiome uniqueness score, women showed a nearly 50% greater  $\beta$ -  
137 coefficient compared to men (adj.  $\beta$  (95%CI): men= 0.0088 (0.006, 0.012), women= 0.013  
138 (0.010, 0.015), interaction term  $P$ -Value= 0.011), indicating that women's microbiomes become  
139 more unique with age at a significantly faster rate.  
140

141 **Reflection of gut microbial uniqueness in the host metabolome**

142 Our research group has previously demonstrated a strong reflection of gut microbiome  
143 community structure in the human plasma metabolome<sup>21</sup>. In order to better understand how host  
144 physiology reflects the increasingly unique composition of the gut microbiome seen with aging,  
145 and to gain potential mechanistic insight into the functional changes that take place in the  
146 microbiota, we regressed our uniqueness measure against each of the 652 plasma metabolites  
147 measured in the Arivale cohort, adjusting for age, age squared, sex, a sex\*age interaction term,  
148 BMI, vendor and Shannon diversity. A total of eight metabolites, all microbial in origin,  
149 remained significantly associated with uniqueness after multiple hypothesis correction  
150 (Bonferroni  $P$ -Value<0.05) (Fig. 3A&B). These metabolites fell primarily into one of two  
151 classes: phenylalanine/tyrosine metabolites (phenylacetylglutamine, p-cresol glucuronide, p-  
152 cresol sulfate) and tryptophan metabolites (3-indoxyl sulfate, 6-hydroxyindole sulfate and  
153 indoleacetate). Interestingly, significant changes in both tryptophan and phenylalanine pathways  
154 have been previously reported in centenarians relative to younger controls, with centenarians  
155 showing greater activation of these pathways in the gut microbiome<sup>22,23</sup>. The previously  
156 identified longevity biomarker, phenylacetylglutamine<sup>23</sup>, demonstrated the strongest  
157 correspondence with gut microbial uniqueness in our analysis, explaining 8.4% of the variance  
158 (adj.  $\beta$  (95%CI) = 0.015 (0.012,0.018),  $P$ -Value= 3.65e-20) (Fig. 3C, Table S4). These findings  
159 indicate that the observed gut microbial drift towards a more unique compositional state seen  
160 with age is characterized by alterations in microbial amino acid metabolism, which may serve as  
161 a useful biomarker for gut microbiome shifts across the human lifespan.  
162

163 **Gut microbial pattern of healthy aging in latest decades of human life**

164 To better understand the long-term health implications of the identified aging dynamics of the  
165 gut microbiome, we extended our analysis into a separate cohort of older men with paired health  
166 and longitudinal follow-up data (the MrOS cohort). The MrOS study recruited older male  
167 participants across the United States. At the fourth follow-up visit, a subset of the participants  
168 provided stool samples for 16S rRNA sequencing of their gut microbiome (discovery cohort  
169 N=599, validation cohort N=308)<sup>17</sup>. All participants who provided a stool sample exceeded 78  
170 years of age at the time of sampling, allowing us to gain insight into the relationship between the  
171 gut microbiome and host health at the latest decades of human life (Fig.1 & Table S2). Once  
172 again, we calculated a uniqueness score for each individual using the Bray-Curtis dissimilarity  
173 metric. Projecting MrOS microbiome data onto the first two Principal Coordinates revealed that  
174 samples with the highest Bray-Curtis uniqueness tended to fall away from common microbiome  
175 profiles, i.e. *Bacteroides* or *Prevotella* dominated ecosystems (Fig. 4A-C). In fact, the relative  
176 abundance of *Bacteroides* showed a strong negative association with gut microbiome uniqueness  
177 (Spearman Rho=0.73, Fig. 4D). The association was even more pronounced when the sum of  
178 both *Bacteroides* and *Prevotella* abundances for each individual was compared to gut  
179 microbiome uniqueness (Spearman Rho=0.80, Figure S1A).

180 Consistent with our initial analysis, age showed a trending positive association with our  
181 uniqueness score in the MrOS cohort (Pearson's  $r$ =0.075,  $P$ -Value= 0.065). Unlike the Arivale

182 cohort, MrOS participants were considerably more health heterogenous at time of sampling, with  
183 a large proportion of participants reporting chronic conditions (**Table S2**). The large health  
184 heterogeneity of MrOS participants provided an opportunity to better understand whether the  
185 observed increase in microbiome dissimilarity with age depends on host health. Hence, we re-ran  
186 the above analysis under four different stratifications based on: medication use, self-perceived  
187 health, life-space score (LSC), and walking speed. We chose these four health metrics because  
188 collectively they encompass a diverse repertoire of health in older populations (**Table 1**).  
189

190 Under all stratifications considered, we observed a stronger positive association between  
191 age and microbiome uniqueness in healthier individuals, while the association was absent  
192 altogether in individuals demonstrating worse health (**Fig. 4E**). We further generated a  
193 composite stratification (composite healthy), where MrOS participants had to meet at least three  
194 of the four criteria outlined above to be classified as healthy (**Table 1 & Table S2**). In this  
195 limited group of 133 individuals we observed an even stronger association between gut microbial  
196 uniqueness and age than under any individual stratification. We replicated the analysis on the  
197 second batch of MrOS gut microbiome samples, which were processed independently several  
198 years apart (validation cohort, N=308), demonstrating very similar results (**Fig. 4E**). We also ran  
199 the same analysis using Weighted UniFrac dissimilarity, and observed high level of congruence  
200 between results (**Fig. S1B**). In contrast, measures of  $\alpha$ -diversity were not significantly associated  
201 with age under any stratification considered (**Fig. S1B**).  
202

### **Gut microbiome and mortality in extreme aging**

203 Next, we focused exclusively on community-dwelling individuals (i.e. excluding participants in  
204 assisted living, nursing homes, and/or who have been hospitalized in the past 12 months) from  
205 the two MrOS data sets, combined together for increased power (N=706) (**Fig. 1**). We performed  
206 genus-level differential abundance analysis to identify genera associated with age in healthy  
207 composite individuals (N=173) and the remainder of the cohort (N=533), separately, adjusting  
208 for batch (discovery/validation) and BMI. In healthy composite individuals, only the genus  
209 *Bacteroides* (adj.  $\beta$  (s.e.): -0.062 (0.017), *P-Value*=0.0006) demonstrated a significant negative  
210 association with age after multiple hypothesis correction (**Fig. 5A**). These findings are consistent  
211 with our gut dissimilarity analysis, where the uniting feature of unique microbiomes is the  
212 depletion of the most common and dominant genera. Consistently, there was no significant  
213 association between age and *Bacteroides* in participants who did not meet our health criteria (adj.  
214  $\beta$  (s.e.): -0.008 (0.009), *P-Value* =0.37) (**Fig. 5A**). In contrast, individuals in worse health  
215 demonstrated a distinct gut microbiome aging pattern characterized by a decline in the genera  
216 *Lachnoclostridium* (adj.  $\beta$  (s.e.): -0.035 (0.0091), *P-Value* =0.0002) and the *Ruminococace*  
217 family genus *UBA1819* (adj.  $\beta$  (s.e.): -0.074 (0.015), *P-Value* =2.57e-06) with age. These results  
218 provide further evidence for the existence of multiple gut microbiome aging patterns in the later  
219 stages of human life.  
220

221 Given that our findings from both  $\beta$ -diversity and differential abundance analysis of  
222 healthy elderly are consistent with observations previously reported in centenarians<sup>4</sup>, we utilized  
223 longitudinal data from the MrOS cohort to investigate whether the observed gut microbiome  
224 pattern of healthy aging is predictive of mortality. We performed the analysis in two steps: 1) on  
225 all community-dwelling participants (N=706) and 2) only on community-dwelling participants in  
226 the top age tertile (85+ years of age, N=257) at time of gut microbiome sampling, because these  
227 participants were the closest to achieving extreme age in the course of the study's follow-up  
period (~4 years). When focusing on all individuals in the cohort, we identified a significant

228 positive association between relative *Bacteroides* abundance and increased risk of all-cause  
229 mortality, independent of age, BMI, clinical site, self-perceived health, diagnosis of congestive  
230 heart failure, and batch in which stool samples were processed. Replicating the analysis in the  
231 oldest individuals (85+ years old) revealed a stronger association and higher Hazard Ratios  
232 compared to the whole cohort (**Fig. 5B-C**). Using the participants' calculated Bray-Curtis  
233 uniqueness score yielded comparable results in 85+ year olds, where mortality risk decreased in  
234 individuals with more unique gut microbiomes independent of the same covariates. In contrast,  
235 the same association between Bray-Curtis uniqueness and mortality was not present when  
236 younger participants were included in the analysis (**Fig. 5C**).  
237

## 238 Discussion

239 There is a limited understanding of how the human gut microbiome changes throughout  
240 adulthood and how these changes influence host physiology. Here, we evaluated gut microbial  
241 patterns associated with aging across 4582 individuals from two distinct study populations  
242 spanning 18-98 years of age. The major findings of our analysis were: 1) individual gut  
243 microbiomes became increasingly more unique with age, starting in mid-to-late adulthood, and  
244 this uniqueness was positively associated with known microbial metabolic markers for health  
245 and longevity; 2) the increase in microbiome uniqueness with age occurred in both males and  
246 females, but was 50% more pronounced in females; 3) in the later decades of human lifespan,  
247 healthy individuals continued to show an increasingly unique gut microbial compositional state  
248 (associated with a decline in core taxa) with age, while that pattern was absent in those in worse  
249 health; 4) in individuals approaching extreme age (85+ years old), retaining high relative  
250 *Bacteroides* abundance and having a low gut microbiome uniqueness score were both associated  
251 with decreased survival in the course of 4 year follow-up. These observations are strengthened  
252 by the presence of similar age-related trends in two separate cohorts, and the replication of  
253 associations with health and longevity in a validation cohort.

254 Our findings indicate that healthy aging of the gut microbiome involves depletion of core  
255 microbes and their replacement by less common taxa, resulting in increasingly distinct  
256 microbiomes. These findings are consistent with patterns previously reported in centenarians  
257 across the world<sup>6,7</sup>, despite the fact that dominant genera (i.e. core microbiota) often vary across  
258 cultures and geographic locations<sup>24</sup>. Using our alternative beta-diversity approach, we provide  
259 novel insight into the aging gut microbiome that a) validates across different vendors and cohorts  
260 and b) is consistent with previous longevity research. It is quite possible that becoming  
261 increasingly dissimilar as you age is a universal characteristic, independent of the variability in  
262 core gut microbes observed across the world (e.g. *Bacteroides* vs. *Prevotella*). This would make  
263 gut microbiome uniqueness an intriguing new dimension of healthy aging, and a critical new  
264 component for personalized medicine and precision health.

265 The reflection of gut microbial uniqueness in plasma phenylalanine/tyrosine and  
266 tryptophan microbial metabolites is consistent with our recent work showing a robust  
267 relationship between the host blood metabolome and gut microbial diversity<sup>21</sup>. Both tryptophan  
268 and phenylalanine metabolism have been implicated in longevity<sup>22,23,25</sup>. Phenylacetylglutamine  
269 and p-cresol sulfate demonstrated some of the strongest associations with gut microbial  
270 uniqueness, independent of age and other covariates. These same metabolites were previously  
271 proposed as biomarkers for healthy aging and longevity<sup>23</sup>. Additional metabolites associated  
272 with our observed gut microbial pattern were dominated by indoles, which are gut microbiome  
273 degradation products of tryptophan. Indoles have been shown to increase healthspan and extend

274 survival in a number of animal models<sup>26</sup>. Their most characterized mechanism of action is  
275 mediating inflammation through binding the aryl hydrocarbon receptor<sup>27</sup>. While further studies  
276 are needed to establish a direct link between these microbial compounds and longevity in  
277 humans, the elevated levels of these metabolites in circulation in individuals whose microbiomes  
278 are more unique opens promising new leads into the role of the gut microbiome in aging.

279 Previous studies in older populations have suggested that gut microbial composition and  
280 structure is generally stable throughout adulthood and into old age<sup>12</sup>, at which point changes are  
281 observed and further accelerated due to adverse health events and lifestyle changes (i.e. entering  
282 long-term care facilities)<sup>10,11,13</sup>. In sharp contrast, our findings suggest that gut microbiomes of  
283 healthy individuals continue to develop throughout aging, and that it is the lack of this  
284 development that appears to be associated with worse health and prognosis. As our  
285 understanding of the aging microbiome increases, monitoring and identifying modifiable features  
286 that may promote healthy aging and longevity will have important clinical implications for the  
287 world's growing older population.

288

## 289 References:

- 290 1. Duvallet, C., Gibbons, S. M., Gurry, T., Irizarry, R. A. & Alm, E. J. Meta-analysis of gut  
291 microbiome studies identifies disease-specific and shared responses. *Nat. Commun.*  
292 (2017). doi:10.1038/s41467-017-01973-8
- 293 2. Koh, A. *et al.* Microbially Produced Imidazole Propionate Impairs Insulin Signaling  
294 through mTORC1. *Cell* (2018). doi:10.1016/j.cell.2018.09.055
- 295 3. Tierney, B. T. *et al.* The predictive power of the microbiome exceeds that of genome-wide  
296 association studies in the discrimination of complex human disease. *bioRxiv*  
297 2019.12.31.891978 (2020). doi:10.1101/2019.12.31.891978
- 298 4. Biagi, E. *et al.* Gut Microbiota and Extreme Longevity. *Curr Biol* **26**, 1480–1485 (2016).
- 299 5. Kim, B. S. *et al.* Comparison of the Gut Microbiota of Centenarians in Longevity Villages  
300 of South Korea with Those of Other Age Groups. *J. Microbiol. Biotechnol.* (2019).  
301 doi:10.4014/jmb.1811.11023
- 302 6. Wu, L. *et al.* A Cross-Sectional Study of Compositional and Functional Profiles of Gut  
303 Microbiota in Sardinian Centenarians. *mSystems* **4**, (2019).
- 304 7. Kong, F. *et al.* Gut microbiota signatures of longevity. *Current Biology* (2016).  
305 doi:10.1016/j.cub.2016.08.015
- 306 8. Kong, F., Deng, F., Li, Y. & Zhao, J. Identification of gut microbiome signatures  
307 associated with longevity provides a promising modulation target for healthy aging. *Gut*  
308 *Microbes* (2019). doi:10.1080/19490976.2018.1494102
- 309 9. Claesson, M. J. *et al.* Composition, variability, and temporal stability of the intestinal  
310 microbiota of the elderly. *Proc Natl Acad Sci U S A* **108 Suppl**, 4586–4591 (2011).
- 311 10. O'Toole, P. W. & Jeffery, I. B. Gut microbiota and aging. *Science* (80- ). **350**, 1214–1215  
312 (2015).
- 313 11. Jeffery, I. B., Lynch, D. B. & O'Toole, P. W. Composition and temporal stability of the  
314 gut microbiota in older persons. *ISME J* **10**, 170–182 (2016).

315 12. Yatsunenko, T. *et al.* Human gut microbiome viewed across age and geography. *Nature*  
316 **486**, 222–227 (2012).

317 13. Jackson, M. *et al.* Signatures of early frailty in the gut microbiota. *Genome Med.* (2016).  
318 doi:10.1186/s13073-016-0262-7

319 14. Salosensaari, A. *et al.* Taxonomic Signatures of Long-Term Mortality Risk in Human Gut  
320 Microbiota. *medRxiv* 2019.12.30.19015842 (2020). doi:10.1101/2019.12.30.19015842

321 15. Zubair, N. *et al.* Genetic Predisposition Impacts Clinical Changes in a Lifestyle Coaching  
322 Program. *Sci. Rep.* (2019). doi:10.1038/s41598-019-43058-0

323 16. Blank, J. B. *et al.* Overview of recruitment for the osteoporotic fractures in men study  
324 (MrOS). *Contemp. Clin. Trials* (2005). doi:10.1016/j.cct.2005.05.005

325 17. Abrahamson, M., Hooker, E., Ajami, N. J., Petrosino, J. F. & Orwoll, E. S. Successful  
326 collection of stool samples for microbiome analyses from a large community-based  
327 population of elderly men. *Contemp. Clin. Trials Commun.* (2017).  
328 doi:10.1016/j.conc.2017.07.002

329 18. Austad, S. N. & Fischer, K. E. Sex Differences in Lifespan. *Cell Metabolism* (2016).  
330 doi:10.1016/j.cmet.2016.05.019

331 19. Ostan, R. *et al.* Gender, aging and longevity in humans: An update of an  
332 intriguing/neglected scenario paving the way to a gender-specific medicine. *Clin. Sci.*  
333 (2016). doi:10.1042/CS20160004

334 20. Lehallier, B. *et al.* Undulating changes in human plasma proteome across lifespan are  
335 linked to disease. *bioRxiv* (2019). doi:10.1101/751115

336 21. Wilmanski, T. *et al.* Blood metabolome predicts gut microbiome  $\alpha$ -diversity in humans.  
337 *Nat. Biotechnol.* (2019). doi:10.1038/s41587-019-0233-9

338 22. Rampelli, S. *et al.* Functional metagenomic profiling of intestinal microbiome in extreme  
339 ageing. *Aging (Albany, NY)*. (2013). doi:10.18632/aging.100623

340 23. Collino, S. *et al.* Metabolic Signatures of Extreme Longevity in Northern Italian  
341 Centenarians Reveal a Complex Remodeling of Lipids, Amino Acids, and Gut Microbiota  
342 Metabolism. *PLoS One* (2013). doi:10.1371/journal.pone.0056564

343 24. Vangay, P. *et al.* US Immigration Westernizes the Human Gut Microbiome. *Cell* (2018).  
344 doi:10.1016/j.cell.2018.10.029

345 25. Ruiz-Ruiz, S. *et al.* Functional microbiome deficits associated with ageing: Chronological  
346 age threshold. *Aging Cell* (2019). doi:10.1111/acel.13063

347 26. Sonowal, R. *et al.* Indoles from commensal bacteria extend healthspan. *Proc. Natl. Acad.*  
348 *Sci. U. S. A.* (2017). doi:10.1073/pnas.1706464114

349 27. Krishnan, S. *et al.* Gut Microbiota-Derived Tryptophan Metabolites Modulate  
350 Inflammatory Response in Hepatocytes and Macrophages. *Cell Rep.* (2018).  
351 doi:10.1016/j.celrep.2018.03.109

352 28. Maier, L. *et al.* Extensive impact of non-antibiotic drugs on human gut bacteria. *Nature*  
353 (2018). doi:10.1038/nature25979

354 29. Charlesworth, C. J., Smit, E., Lee, D. S. H., Alramadhan, F. & Odden, M. C.  
355 Polypharmacy among adults aged 65 years and older in the United States: 1988â"2010.  
356 *Journals of Gerontology - Series A Biological Sciences and Medical Sciences* (2015).  
357 doi:10.1093/gerona/glv013

358 30. Machón, M., Vergara, I., Dorronsoro, M., Vrotsou, K. & Larrañaga, I. Self-perceived  
359 health in functionally independent older people: Associated factors. *BMC Geriatr.* (2016).  
360 doi:10.1186/s12877-016-0239-9

361 31. Idler, E. L. & Benyamin, Y. Self-Rated Health and Mortality: A Review of Twenty-  
362 Seven Community Studies. *Journal of Health and Social Behavior* (1997).  
363 doi:10.2307/2955359

364 32. Mossey, J. M. & Shapiro, E. Self-rated health: a predictor of mortality among the elderly.  
365 *Am. J. Public Health* (1982). doi:10.2105/AJPH.72.8.800

366 33. Mackey, D. C. *et al.* Life-space mobility and mortality in older men: A prospective cohort  
367 study. *J. Am. Geriatr. Soc.* (2014). doi:10.1111/jgs.12892

368 34. Peel, C. *et al.* Assessing Mobility in Older Adults: The UAB Study of Aging Life-Space  
369 Assessment. *Phys. Ther.* (2005). doi:10.1093/ptj/85.10.1008

370 35. Middleton, A., Fritz, S. L. & Lusardi, M. Walking speed: The functional vital sign.  
371 *Journal of Aging and Physical Activity* (2015). doi:10.1123/japa.2013-0236

372 36. Mielke, M. M. *et al.* Assessing the temporal relationship between cognition and gait: Slow  
373 gait predicts cognitive decline in the mayo clinic study of aging. *Journals Gerontol. - Ser.*  
374 *A Biol. Sci. Med. Sci.* (2013). doi:10.1093/gerona/gls256

375 37. Manor, O. *et al.* A Multi-omic Association Study of Trimethylamine N-Oxide. *Cell Rep.*  
376 (2018). doi:10.1016/j.celrep.2018.06.096

377 38. Callahan, B. J. *et al.* DADA2: High-resolution sample inference from Illumina amplicon  
378 data. *Nat Methods* **13**, 581â"583 (2016).

379 39. Wright, E. S. DECIPHER: Harnessing local sequence context to improve protein multiple  
380 sequence alignment. *BMC Bioinformatics* (2015). doi:10.1186/s12859-015-0749-z

381 40. Price, M. N., Dehal, P. S. & Arkin, A. P. FastTree 2 - Approximately maximum-  
382 likelihood trees for large alignments. *PLoS One* (2010).  
383 doi:10.1371/journal.pone.0009490

384 41. McMurdie, P. J. & Holmes, S. Phyloseq: An R Package for Reproducible Interactive  
385 Analysis and Graphics of Microbiome Census Data. *PLoS One* (2013).  
386 doi:10.1371/journal.pone.0061217

387 42. Bray, J. R. & Curtis, J. T. An Ordination of the Upland Forest Communities of Southern  
388 Wisconsin. *Ecol. Monogr.* (1957). doi:10.2307/1942268

389 43. Lozupone, C. & Knight, R. UniFrac: A new phylogenetic method for comparing microbial  
390 communities. *Appl. Environ. Microbiol.* (2005). doi:10.1128/AEM.71.12.8228-8235.2005

391 44. Edgar, R. C. UPARSE: Highly accurate OTU sequences from microbial amplicon reads.  
392 *Nat. Methods* (2013). doi:10.1038/nmeth.2604

393 45. Quast, C. *et al.* The SILVA ribosomal RNA gene database project: Improved data

394  
395  
396  
397

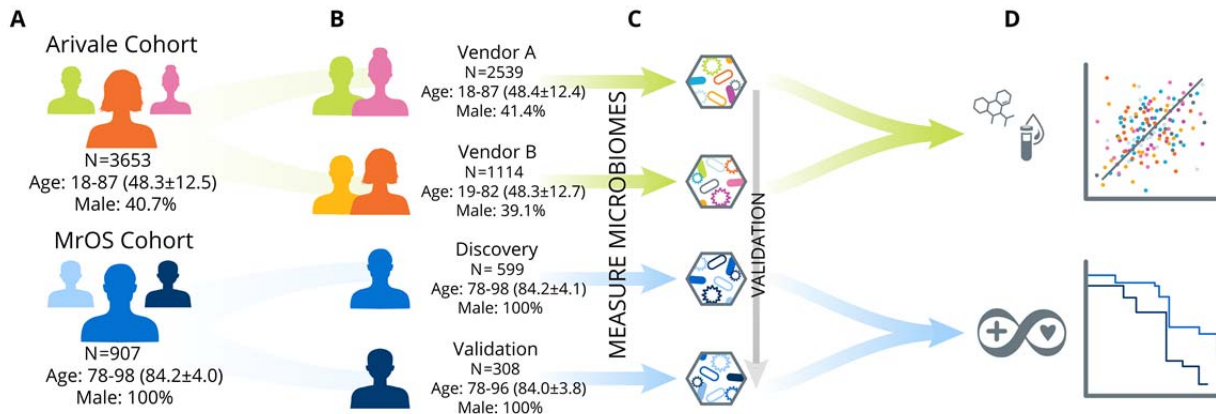
processing and web-based tools. *Nucleic Acids Res.* (2013). doi:10.1093/nar/gks1219

46. Martin, B. D., Witten, D. & Willis, A. D. Modeling microbial abundances and dysbiosis with beta-binomial regression. *arXiv* 1902.02776 (2019).

Health Metric	Description	Stratification
Medication use	Medication use is associated with chronic diseases and comorbidities, and is an important modulator of the gut microbiome <sup>28</sup> . High medication use is particularly prevalent in older populations, with nearly 40% of individuals 65+ years old reporting taking $\geq 5$ medications <sup>29</sup> .	High: $>8$ , Low: $\leq 8$ medications. This allowed us to generate two groups of participants with similar age distribution but very different pharmacological profiles (low-med: N=292; high-med: N=307). Despite no significant differences in age between these two groups (student's t-test, <i>P-Value</i> =0.33), the prevalences of several diseases, including diabetes, chronic obstructive pulmonary disease, and congestive heart failure, were significantly higher in individuals reporting high number of medications ( <b>Table S5</b> ).
Self-perceived health	Self-perceived health has been previously shown to be an independent predictor of earlier mortality in older populations <sup>30-32</sup> .	In the MrOS cohort, individuals chose one out of five possible responses (excellent, good, fair, poor, very poor). We stratified the cohort into individuals who reported excellent health (N=205) and those who reported anything less than excellent (N=394).
Life-space Score (LSC)	LSC is an indicator of mobility, i.e. how often an individual leaves their room, house, or neighborhood and has been previously associated with risk of mortality in MrOS participants <sup>33</sup> . Its strength as a measure lies in that it not only provides insight into whether an individual is physically <i>capable</i> of performing activities, but also whether that individual <i>actually</i> performs these activities <sup>34</sup> .	For both the LSC and walking speed, we stratified the cohort into tertiles and defined the top tertile as the healthy group (High), while the bottom two tertiles were combined into the less healthy group (low).
Walking Speed	Walking speed is a validated measure used to assess functional status and overall health <sup>35</sup> , and had been previously shown to be associated with executive function, and predictive of cognitive decline <sup>36</sup> .	
Composite	A composite of all 4 of the above measures	Healthy - individuals who met 3+ of the above criteria

398

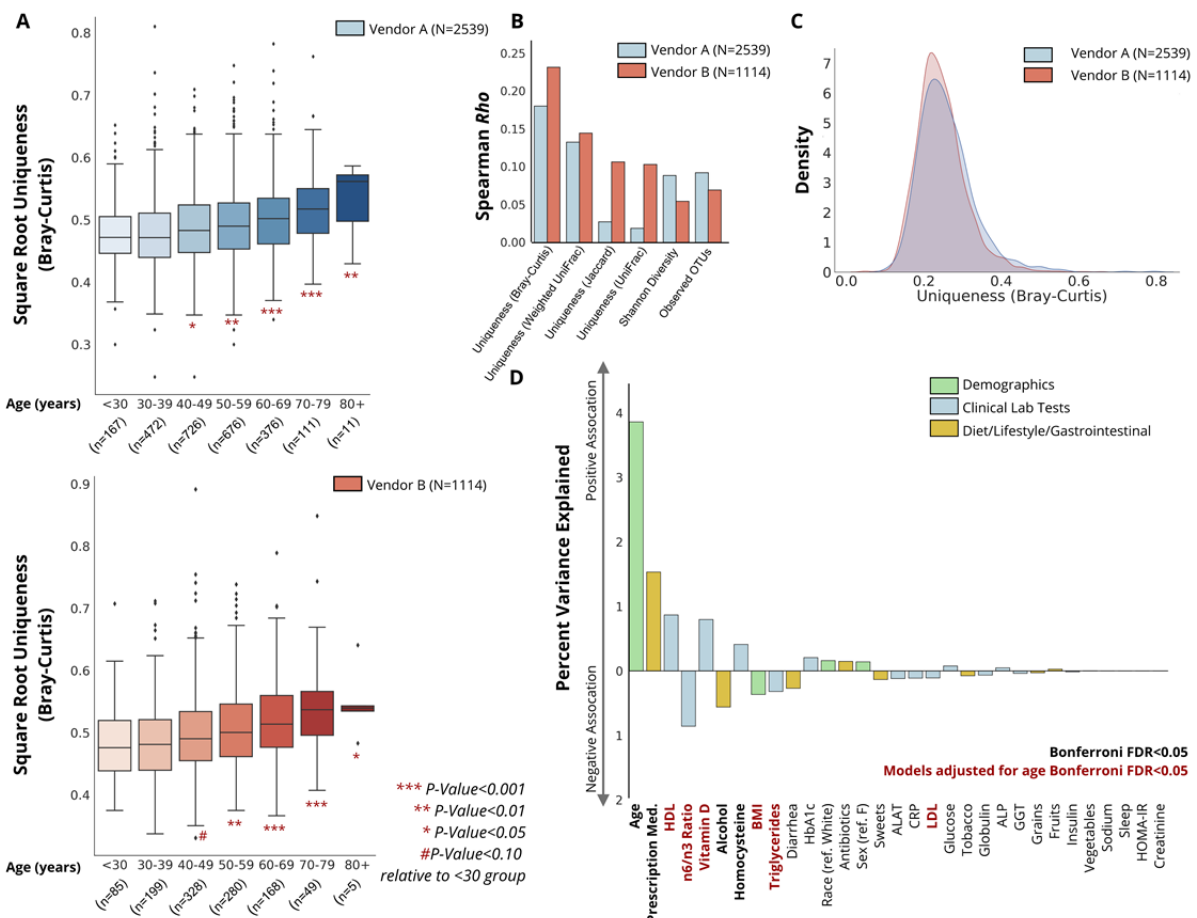
**Table 1: Description of health metrics used for stratification in the MrOS cohort.**



399

400 **Fig. 1. Conceptual outline of study and analysis workflow.** (A) Two different study  
401 populations were used: the Arivale cohort and the Osteoporotic Fractures in Men (MrOS) cohort.  
402 (B) Each of these two study populations were further subdivided into two groups; the Arivale  
403 cohort was split based on the microbiome vendor used to collect and process samples while the  
404 MrOS cohort separated into Discovery and Validation groups based on the batch in which the  
405 samples were run (discovery samples were processed in the initial batch, validation samples were  
406 processed several years later). (C) We profiled the microbiomes from these four study  
407 populations beginning with the Arivale cohort and validating our findings across the three  
408 additional populations. (D) Our analysis pipeline further explored associations between the  
409 identified gut microbial aging pattern, lifestyle factors, and host physiology in the combined  
410 Arivale cohort, as well as health metrics and mortality in the combined MrOS cohort.

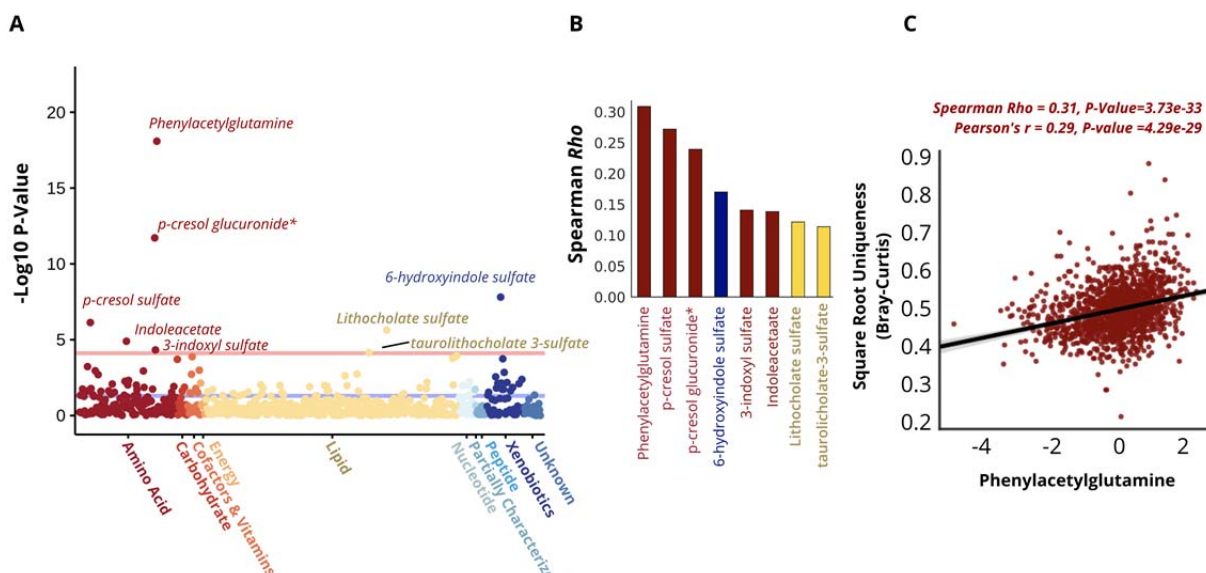
411



412

## 413 Fig. 2. Associations between gut microbial uniqueness and age across the Arivale cohort.

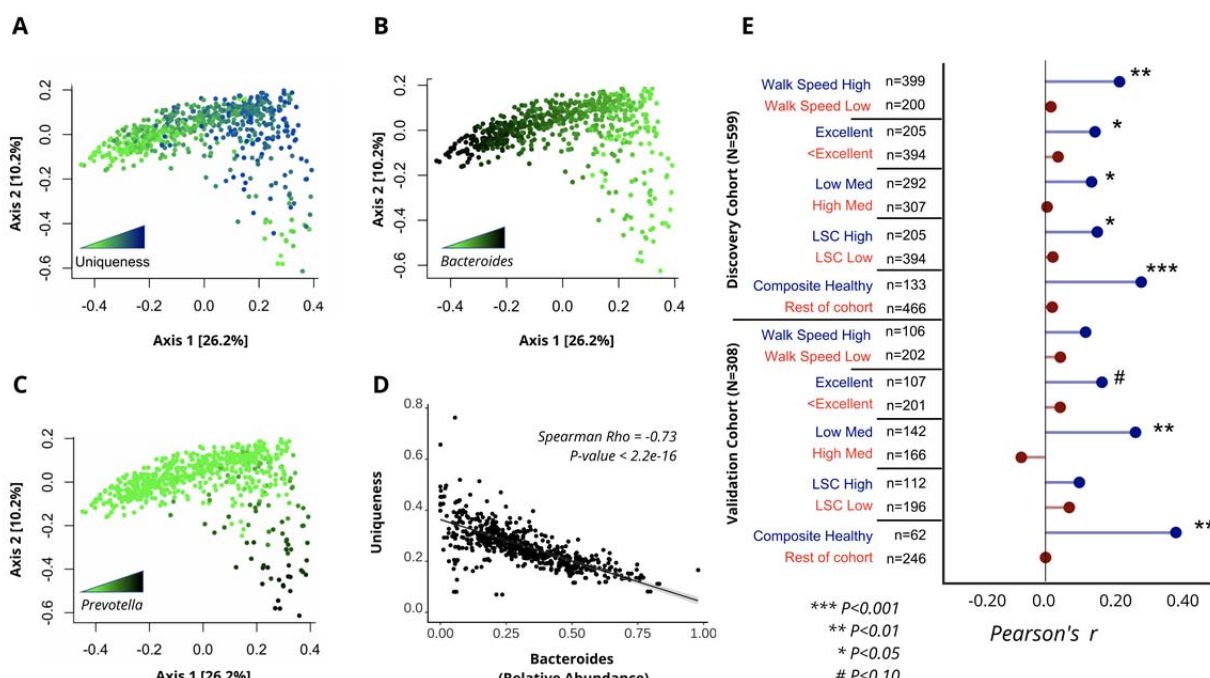
414 (A) Boxplots showing gut microbiome uniqueness scores calculated using the Bray-Curtis  
415 dissimilarity metric across the adult lifespan in individuals whose stool samples were collected  
416 and processed by vendor A (blue) or B (red). Asterisks indicate significant differences relative to  
417 the youngest <30 group, from a linear regression model adjusted for sex, BMI, and Shannon  
418 diversity. Box plots represent the interquartile range (25th to 75th percentile, IQR), with the  
419 middle line demarking the median; whiskers span  $1.5 \times$  IQR, points beyond this range are shown  
420 individually. (B) Spearman correlation coefficients for measures of uniqueness ( $\beta$ -diversity) and  
421  $\alpha$ -diversity with age in individuals whose stool samples were processed by vendor A or B. (C)  
422 Distribution of uniqueness calculated using the Bray-Curtis metric in each of the two vendors.  
423 (D) Percent of variance explained in Bray-Curtis uniqueness by a diverse number of  
424 demographic and lifestyle factors, as well as a subset of clinical laboratory tests.



425  
426  
427  
428  
429  
430  
431  
432  
433  
434  
435  
436  
437  
438

**Fig. 3. Reflection of gut microbiome uniqueness in plasma metabolites.** (A) A plot of  $-\log_{10}$  p-values for each of the 652 plasma metabolites measured in the Arivale cohort, from OLS regression models predicting Bray-Curtis uniqueness adjusted for age, age squared, sex, an age\*sex interaction term, BMI, Shannon diversity and microbiome vendor. Metabolites are color-coded by their super-family. All metabolites above the red line are significant after multiple-hypothesis correction (Bonferroni  $P<0.05$ ). \* indicates metabolites that were confidently identified on the basis of mass spectrometry data, but for which no reference standards are available to verify the identity. (B) Spearman correlation coefficients for each of the metabolites significantly associated with Bray-Curtis uniqueness after adjusting for covariates and multiple-hypothesis correction (Bonferroni  $P<0.05$ ). Bars are color-coded as in A). (C) Scatter plot of Bray-Curtis Uniqueness and the strongest metabolite predictor, phenylacetylglutamine. The line shown is a  $y \times x$  regression line, and the shaded regions are 95% confidence intervals for the slope of the line.

439



440

441

**Fig. 4. Increased dissimilarity of the gut microbiome as a function of healthy aging in the MrOS Cohort.** (A-C) PCoA of the MrOS discovery cohort color-coded by (A) Bray-Curtis uniqueness, (B) relative *Bacteroides* abundance, and (C) relative *Prevotella* abundance. (D) Scatter plot demonstrating the negative association of the relative abundance of the most dominant genus *Bacteroides* and gut microbial uniqueness in the discovery cohort. The line shown is the y~x regression line, while the shaded region corresponds to the 95% confidence intervals for the slope of the line. (E) Correlation of Bray-Curtis uniqueness scores with age across the MrOS discovery and validation cohorts under different health stratifications. ‘Excellent’ corresponds to individuals who self-reported their health to be excellent, while ‘<Excellent’ incorporates all individuals who self-reported their health being anything less than excellent (good, fair, poor, or very poor). ‘Composite Healthy’ refers to individuals who fell into the healthy sub-group in at least 3 of the 4 stratifications performed. LSC: Life-Space Score.

452

453

454

455

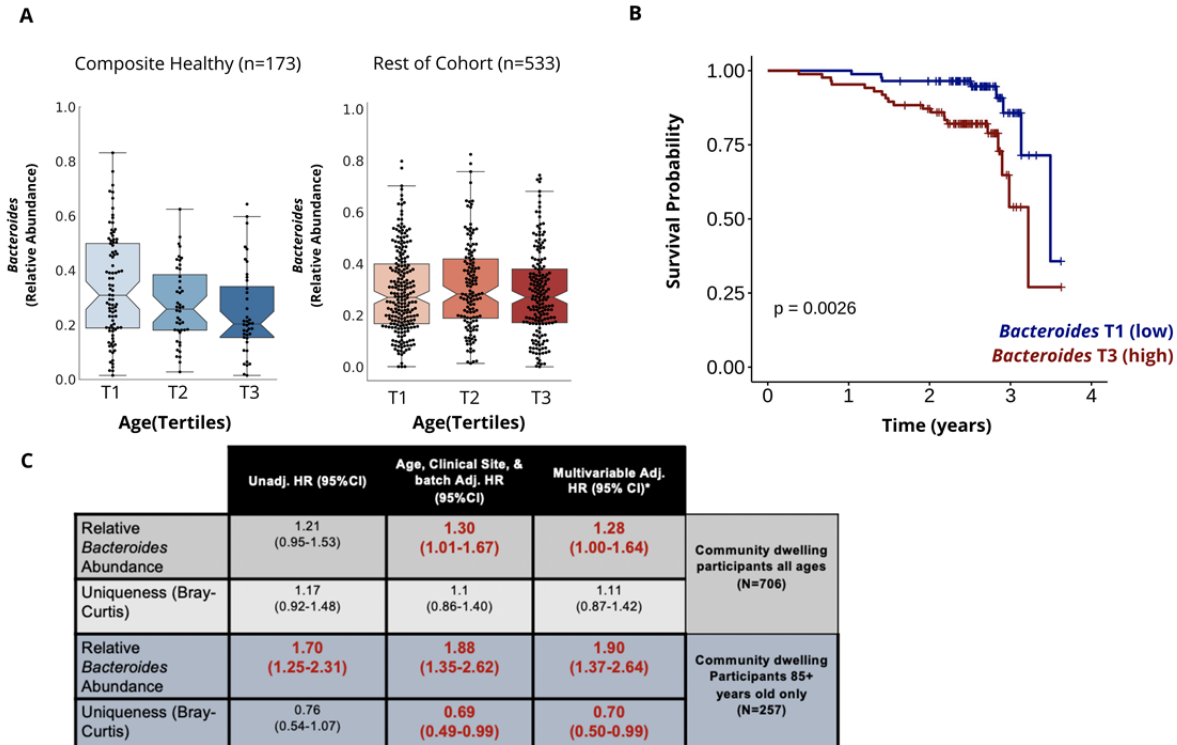


**Figure 5. Association of *Bacteroides* abundance and survival in latter decades of human lifespan.** (A) Boxplots demonstrating the relative abundance of the genus *Bacteroides* across tertiles of age in community-dwelling individuals identified as healthy on 3+ criteria specified (composite healthy) (n=173) and the remainder of the cohort (n=533). (B) Kaplan Meier Curve demonstrating the association between overall survival and relative *Bacteroides* abundance grouped into tertiles in community-dwelling MrOS participants who were 85+ years at time of sampling (N=257). (C) Unadjusted, age, clinical site and batch adjusted and multivariable adjusted Hazard Ratios (HR) of relative *Bacteroides* abundance and Bray-Curtis Uniqueness scores from Cox Proportional Hazard Regression models evaluating mortality risk in all community-dwelling MrOS participants and exclusively community-dwelling MrOS participants 85+ years old. Multivariable models were adjusted for age, clinical site, BMI, self-perceived health, diagnosis of congestive heart failure, and batch in which stool samples were processed. Both relative *Bacteroides* abundance and The Bray-Curtis uniqueness measures were scaled and centered prior to mortality analysis. Significant HRs are bolded and colored in red ( $P \leq 0.05$ ).

456

457

458

459

460

461

462

463

464

465

466

467

468

469

470

471

472

473

474

475

476

477

478

479

480

481

482

483 **Acknowledgments:** We thank C. Funk for helpful discussions throughout the course of this  
484 project. We also thank J. Dougherty and M. Brunkow for their coordination efforts. **Funding:**  
485 This work was supported by the M.J. Murdock Charitable Trust (L.H. and N.D.P.), Arivale and a  
486 generous gift from C. Ellison. S.M.G., C.D. and S.P. were supported by a Washington Research  
487 Foundation Distinguished Investigator Award and by start-up funds from the Institute for  
488 Systems Biology. The Osteoporotic Fractures in Men (MrOS) Study is supported by National  
489 Institutes of Health funding. The following institutes provide support: the National Institute on  
490 Aging (NIA), the National Institute of Arthritis and Musculoskeletal and Skin Diseases  
491 (NIAMS), the National Center for Advancing Translational Sciences (NCATS), and NIH  
492 Roadmap for Medical Research under the following grant numbers: U01 AG027810, U01  
493 AG042124, U01 AG042139, U01 AG042140, U01 AG042143, U01 AG042145, U01  
494 AG042168, U01 AR066160, and UL1 TR000128. **Author contributions:** T.W., S.M.G., L.H.,  
495 E.S.O., and N.P conceptualized the study. T.W., J.W., J.L., J.A.C., S.M.G., and E.S.O  
496 participated in study design. T.W., C.D., N.R., S.P., J.W., J.L., J.C.E., A.Z., and J.T.Y.  
497 performed data analysis and figure generation. G.G. and M.R. aided in dissimilarity analysis.  
498 G.G., M.R., N.E.L., J.Z., J.A.C and D.M.K. assisted in results interpretation. A.T.M. and J.L.  
499 managed the logistics of data collection and integration. T.W., S.M.G., E.S.O and N.P. were the  
500 primary writers of the paper, with contributions from all authors. All authors read and approved  
501 the final manuscript. **Competing interests:** Authors declare no competing interests. **Data and**  
502 **materials availability:** Qualified researchers can access the full Arivale deidentified dataset  
503 analyzed in this study for research purposes. Requests should be sent to  
504 [nathan.price@isbscience.org](mailto:nathan.price@isbscience.org). The MrOS data set is available to researchers through the  
505 following website: <https://mrosdata.sfcc-cpmc.net>.

506  
507  
508 **Methods:**

509 **Cohorts:** The Arivale cohort consists of individuals over 18 years of age who between 2015 and  
510 2019 self-enrolled in a now closed scientific wellness company. The cohort has been described  
511 in detail previously<sup>15</sup>. For this study, only baseline measurements were considered for each  
512 participant. The only inclusion criterion was the availability of gut microbiome data in order to  
513 maximize the number of gut microbiomes to which each sample is compared. Demographic  
514 information on the cohort is provided in Table S1.

515 The MrOS study is an ongoing prospective study of close to 6000 men recruited across six  
516 clinical U.S. sites. The cohort, recruitment criteria, and stool sample collections have been  
517 previously described in detail<sup>16,17</sup>. Briefly, during the fourth follow-up visit of the original study,  
518 a subset of participants across all six clinics was asked if they would consent to have their stool  
519 sampled for microbiome analysis. Participants who agreed were given the OMNIgene-GUT  
520 stool/feces collection kit (OMR-200, DNA Genotek, Ottawa, Canada) and collected the fecal  
521 sample at their homes. Demographic information on MrOS participants is provided in Table S2.  
522 In the initial uniqueness analysis, all participants with available high-quality microbiome data  
523 were used for analysis (N=907). Subsequent differential abundance analysis focused exclusively  
524 on community-dwelling individuals (N=706) (excluding individuals in assisted living, nursing  
525 homes and who have been hospitalized in the past 12 months). Finally, survival analysis was  
526 conducted on all community dwelling individuals as well as specifically on community dwelling  
527 individuals in the latest stages of aging (85+ years old, N=257). The number of deaths in the

528 whole community dwelling group and in 85+ year old community dwelling group was 66 and  
529 41, respectively.

530 **Microbiome Analysis:**

531 **Arivale cohort:** Analysis of gut microbiome data from the Arivale cohort has been described in  
532 detail elsewhere<sup>21,37</sup>. Briefly, independent of the vendor used, stool samples were collected at  
533 the participants' homes using DNA collection kits with a proprietary chemical DNA stabilizer to  
534 maintain DNA integrity at ambient temperatures following collection. Gut microbiome  
535 sequencing data in the form of FASTQ files were provided on the basis of either the 300-bp  
536 paired-end MiSeq profiling of the 16S V3 + V4 region (DNAGenotek, vendor A) or 250-bp  
537 paired-end MiSeq profiling of the 16S V4 region (Second Genome, vendor B). Further analysis  
538 was performed using the denoise workflow from mbtools (<https://github.com/gibbons-lab/mbtools>) that wraps DADA2<sup>38</sup> error models  
539 separately for each sequencing run and used those to obtain sequence variants for each sample.  
540 This was followed by de novo chimera removal which removed ~17% of all reads as chimeric  
541 and resulted in about 89,000 final sequence variants across all samples. Taxonomy assignment  
542 was performed using the RDP classifier with the SILVA database (version 132). Here 99% of the  
543 reads could be classified on the family level, 89% on the genus level and 32% on the species  
544 level. Species level taxonomy was identified by exact alignment to the SILVA reference  
545 sequences. Sequence variants were aligned to each other using DECIPHER<sup>39</sup> and the multiple  
546 sequence alignment was trimmed by removing each position that consisted of more than 50%  
547 gaps. The resulting core alignment had a length of 420 base pairs and was used to reconstruct a  
548 phylogenetic tree using FastTree<sup>40</sup>. Downstream gut microbiome data analysis was conducted  
549 using the *Phyloseq* Package<sup>41</sup>. In two separate analyses, gut microbiome samples were rarefied  
550 to 13703 (vendor A, DNAGenotek) and 39810 (Vendor B, Second Genome) reads, the minimum  
551 number of reads per sample for each vendor. For uniqueness analysis, the Bray-Curtis<sup>42</sup>,  
552 Unweighted and Weighted UniFrac<sup>43</sup>, and Jaccard matrices were calculated for all samples  
553 within each vendor using the rarefied Genus table. The minimum value for each row,  
554 corresponding to the dissimilarity of each sample to their nearest neighbor, was then extracted  
555 from the matrix and used for downstream analysis.

556 **MrOS cohort:** Stool samples were processed at the Alkek Center for Metagenomics and  
557 Microbiome Research (CMMR) at Baylor College of Medicine using their custom analytic  
558 pipeline in two separate batches (Discovery N=599, Validation N=320). 16Sv4 rDNA amplicon  
559 sequences were clustered into Operational Taxonomic Units (OTUs) at a similarity cutoff value  
560 of 97% using the UPARSE algorithm<sup>44</sup>. OTUs were then mapped to an optimized version of the  
561 SILVA Database<sup>45</sup> containing only the 16S V4 region to determine taxonomies. Abundances  
562 were recovered by mapping the demultiplexed reads to the UPARSE OTUs<sup>44</sup>. Preliminary  
563 microbiome data analysis was conducted using the *Phyloseq* Package. For  $\alpha$ -diversity and  
564 uniqueness analysis, OTUs were rarefied to 9424 reads, which is the minimum number of  
565 OTUs/sample in the discovery cohort. The same rarefaction number (9424) was used in the  
566 Validation cohort (N=320). A total of 12 samples had less reads than the specified cut-off, and  
567 hence were excluded from the analysis (Validation N=308).  $\alpha$ -diversity measures were  
568 calculated at the OTU level using the *Phyloseq* package<sup>41</sup>. For  $\beta$ -diversity analysis, OTUs were  
569 collapsed into genera. Uniqueness was calculated as described for the Arivale cohort. The  
570 calculated uniqueness measure for each participant was then used for downstream analysis. As  
571 part of our analytical pipeline, we also performed differential abundance analysis assessing the  
572 relationship of individual genera with age in individuals defined as healthy and unhealthy,  
573

574 separately. Analysis was performed in R (version 3.44) using beta-binomial regression through  
575 the Corncob package (version 1.0)<sup>46</sup>. Models were adjusted for BMI, and batch  
576 (discovery/validation). Type 1 error was controlled using the Bonferroni method (P<0.1).

577 **Plasma Metabolomics & Clinical Laboratory Tests:**

578 Blood draws for all assays were performed by trained phlebotomists at LabCorp or Quest service  
579 centers. For the 24-hour period leading up to the blood draw, Arivale participants were required  
580 to avoid alcohol, vigorous exercise, aspartame and monosodium glutamate, and to begin fasting  
581 12 hours in advance. Plasma metabolomics assays were conducted on the samples by Metabolon,  
582 Inc. Sample handling, quality control and data extraction, along with biochemical identification,  
583 data curation, quantification and data normalizations have been previously described<sup>37</sup>. For  
584 analysis, the raw metabolomics data were median scaled within each batch, such that the median  
585 value for each metabolite was one. To adjust for possible batch effects, further normalization  
586 across batches was performed by dividing the median-scaled value of each metabolite by the  
587 corresponding average value for the same metabolite in quality control samples of the same  
588 batch. In this study, we analyzed participants' baseline plasma metabolomics data. A 10%  
589 missing value threshold was set, which was passed by 652 metabolites. Missing values for  
590 metabolites were imputed to be the minimum observed value for that metabolite. A total of 1476  
591 Arivale participants had paired gut microbiome-plasma metabolome data. Values for each  
592 metabolite were log transformed prior to analysis. Clinical laboratory tests were conducted by  
593 either Quest or LabCorp. A 10% missing value threshold was set for each clinical laboratory test  
594 used in the analysis. All but 104 participants (N=3549) had paired clinical laboratory-gut  
595 microbiome data. Both metabolomics and clinical laboratory tests were scaled and centered prior  
596 to analysis and only baseline measures for each individual were used.

597 **Lifestyle/Health Questionnaires in the Arivale Cohort:**

598 Data on lifestyle, diet and health were obtained through self-administered questionnaires  
599 completed by Arivale participants during their initial assessment. For reporting antibiotic use,  
600 participants chose from three possible responses ('not in the past year', 'in the past year' and 'in  
601 the past three months') which were recoded into ordinal variables 0, 1 and 2 respectively.  
602 Participants chose one of several possible frequencies in response to how often they experience  
603 diarrhea, that were recoded as follows: 'infrequently/never' = 0, 'once a week or less' = 1, 'more  
604 than once a week' = 2 and 'daily' = 2. Similarly, alcohol use (no. of drinks per day) was reported  
605 on the following scale which was recoded into corresponding ordinal variables: (0) 'I do not  
606 drink', (1) '1-2 drinks': (2) '3-4 drinks': (3) '5-6 drinks': (4) 'More than 6 drinks'. Current tobacco  
607 use and prescription medication were both modelled as binary variables (yes/no). Finally, for  
608 dietary variables (fruit, vegetables, grains, and sweets intake), participants chose one of the  
609 following responses, which were then recoded to the corresponding ordinal variables: (grains):  
610 (0) 'Zero/less than 1 per day': (1) '1-2': (2) '3-4': (3) '5-6': and (4) '7 or more'. (fruits,  
611 vegetables): (0) 'Zero/less than 1 per day': (1) '1': (2) '2-3': (3) '4-5': (4) '6 or more'.  
612 (chocolates/sweets): (0) 'Less than once per month': (1) '1-3 times per month': (2) 'Once per  
613 week': (3) '2-4 times per week': (4) '5-6 times per week': (5) 'Once per day': (6) '2-3 times per  
614 day': (6) '4-5 times per day': (6) '6+ times per day'. Sleep was reported as the average amount of  
615 sleep you get a day on a three-point scale: (0) 'Less than 6 hours': (1) '7 to 9 hours': (2) 'More  
616 than 9 hours'. As the Arivale cohort consists of self-enrolled participants, the response rates for  
617 different questionnaires vary. The number of missing values for each response is reported in  
618 Table S2.

619 **Health Measures in the MrOS Cohort:**

620 We utilized four different health measures that were collected on MrOS participants during their  
621 fourth follow-up visit. Medication use, self-perceived health, and the Life-Space score (LSC)  
622 were all self-reported. Self-perceived health captured each individual's rating of their own health  
623 compared to other individuals their own age. The implementation of the LSC in the MrOS cohort  
624 has been described in detail previously <sup>33</sup>. Briefly, LSC can range from 0 (restricted to one's  
625 bedroom) to 120 (traveled outside one's town daily without assistance). We defined healthy  
626 individuals as those in the top tertile of the LSC cohort distribution. This corresponded to an  
627 LSC value of  $\geq 96$ . Walking speed was calculated based on the time it took each participant to  
628 walk 6 meters (m/s). Like with the LSC, we defined healthy individuals based on walking speed  
629 if their speed was in the top tertile ( $\geq 1.17$ ). A total of 7 MrOS participants did not have available  
630 walking speed data. This is due to either the participants not coming to the clinic, or not being  
631 able to attempt the test. These individuals were classified in the walking speed low group in our  
632 analysis.

### 633 **Statistical Analysis:**

634 Depending on the statistical approach, analysis was conducted using either R (v 3.6) or Python (v  
635 3.7). The relationship between the calculated uniqueness measure and age in the Arivale cohort  
636 was modeled using Ordinary Least Square (OLS) linear regression (Python) where square root  
637 transformed Bray-Curtis uniqueness was modeled as the dependent variable and each age decade  
638 was compared to the youngest reference group (<30 years), adjusting for sex, BMI, and Shannon  
639 diversity. We chose to adjust for Shannon diversity because, in our analysis, it was associated  
640 with both age and microbiome uniqueness (higher alpha diversity makes you more likely to be  
641 unique). We wanted to assess the significance of our dissimilarity pattern independent of changes  
642 in alpha diversity seen with age and previously reported in literature. The same adjustment was  
643 not made for MrOS participants, since Shannon diversity showed no association with age in that  
644 cohort. Pearson/Spearman correlations were also used to assess the strength of the relationship  
645 between different measures of  $\beta$ - and  $\alpha$ -diversity and age across all cohorts using the Python  
646 statistical functions package (scipy.stats). When assessing the relationship between clinical,  
647 lifestyle, and demographic variables with gut microbial uniqueness, Bray-Curtis uniqueness  
648 values greater or less than 3 standard deviations from the mean were removed. OLS linear  
649 regression was then used to assess the individual relationship between each factor and square  
650 root transformed Bray-Curtis gut microbial uniqueness, with microbiome vendor included as a  
651 covariate. Percent variance explained by each factor was calculated by taking the percent  
652 variance explained by the complete OLS model (variable of interest and microbiome vendor) and  
653 subtracting the percent variance explained by microbiome vendor alone. The same analysis was  
654 then repeated with age included as a covariate (age-adjusted models). To investigate potential  
655 effect modification of sex on the identified gut microbiome aging pattern, an OLS model was  
656 generated with a sex\*age interaction term predicting square root transformed Bray-Curtis  
657 uniqueness, adjusted for sex, age, BMI, microbiome vendor and Shannon diversity. Sex-specific  
658  $\beta$ -coefficients were estimated by first stratifying the cohort by sex and then fitting OLS models  
659 for men and women separately, adjusting for the same covariates as the combined model. Age  
660 was scaled and centered prior to this analysis. When investigating the relationship between  
661 plasma metabolite concentrations and gut microbial uniqueness, each metabolite was log  
662 transformed and subsequently scaled and centered. The square root transformed Bray-Curtis  
663 uniqueness score was then regressed against each metabolite individually, adjusting for  
664 microbiome vendor, sex, age, age<sup>2</sup>, a sex\*age interaction term, BMI, and Shannon diversity  
665 using OLS regression. In each instance where multiple hypotheses were tested, type I error was

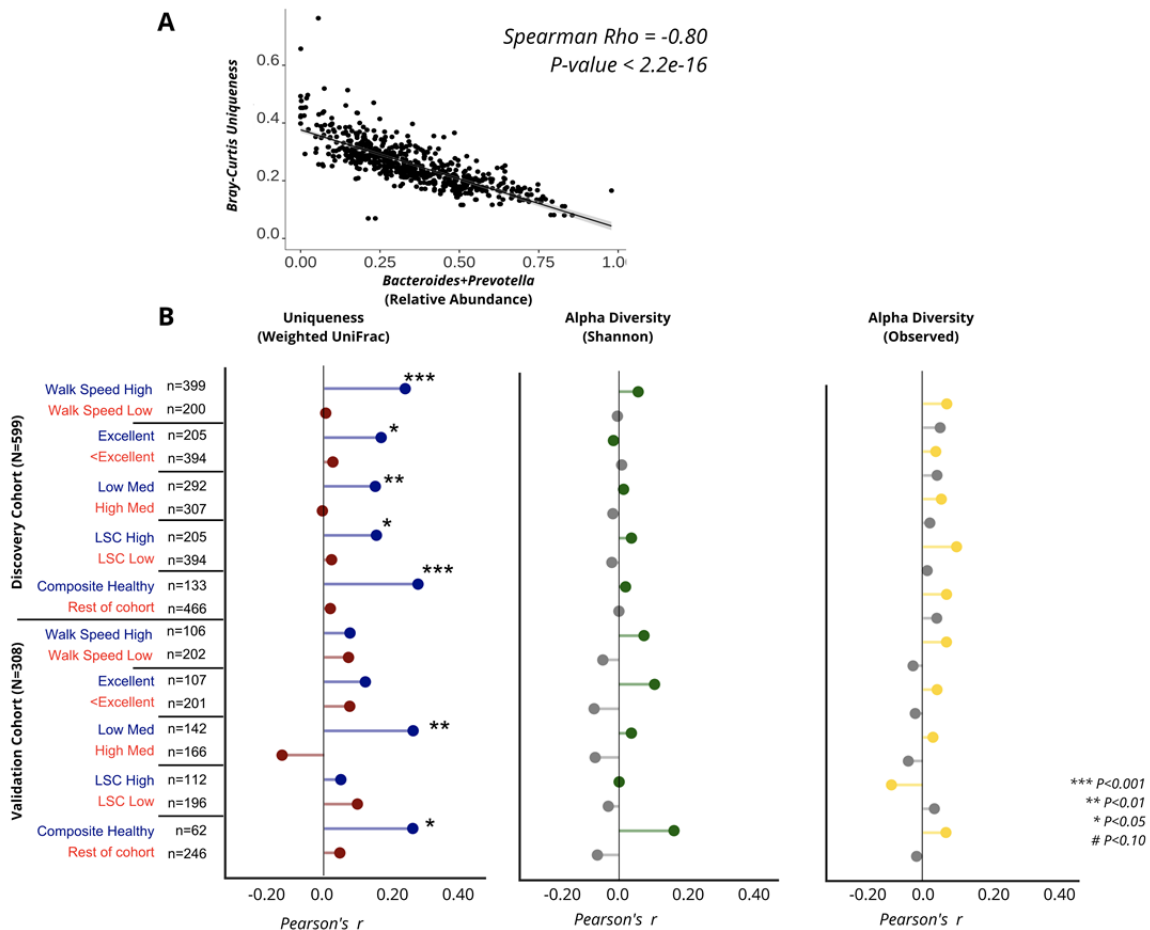
666 controlled for using the Bonferroni method ( $P<0.05$ ). In the MrOS Cohort, correlation between  
 667 Bray-Curtis Uniqueness and age was calculated using the Python statistical functions package  
 668 (scipy.stats) using the square root transformed uniqueness score. Mortality analysis was  
 669 conducted in R using the package survival (v 2.44-1.1). Relative *Bacteroides* abundance (after  
 670 rarefaction) and uniqueness scores were scaled and centered prior to survival analysis. Cox-  
 671 proportional hazard regression models were generated assessing the relationship between  
 672 survival and Relative *Bacteroides* abundance or Bray-Curtis uniqueness independently, adjusting  
 673 for clinical site, batch (discovery/validation) and age, and adjusting for clinical site, age, BMI,  
 674 self-perceived health (excellent, good, <good), diagnosis of congestive heart failure, and batch in  
 675 which stool samples were processed (discovery/validation).  
 676  
 677  
 678  
 679  
 680

681 **Supplementary Information:**

682 Figure S1

683 Tables S1-S5

684



685

686  
687  
688  
689  
690  
691  
692  
693  
694  
695  
696  
697  
698  
699  
700  
701  
702  
703  
704  
705

**Fig. S1. Associations between age and gut microbiome measures across health stratifications in the MrOS cohort.** **(A)** Scatter plot demonstrating the negative association of the relative abundance of the sum of *Bacteroides*+*Prevotella* and gut microbial uniqueness. The line shown is the y~x regression line, while the shaded region corresponds to the 95% confidence intervals for the slope of the line. **(B)** Plots demonstrating the strength of correlation between age and gut microbiome measures. The blue/red panel corresponds to the calculated Weighted UniFrac ( $\beta$ -diversity) uniqueness score, while the grey/green and grey/yellow panels correspond to Shannon diversity and Observed species ( $\alpha$ -diversity measures), respectively. Significant correlations are indicated with pound signs and asterisks.

	<b>Vendor A (N=2539)</b>	<b>Vendor B (N=1114)</b>	<b>P-Value</b>
Mean age (range)	48.4 (18-87)	48.3 (19-82)	NS
Mean BMI (s.d.)	27.1 (5.9)	27.3 (6.1)	NS
Sex (% female)	58.60%	60.90%	NS
Non-white (%)	20.40%	22.00%	NS
Mean HDL (mg dl <sup>-1</sup> ) (s.d.)	61.8 (18.8)	61.7 (18.4)	NS
Mean LDL (mg dl <sup>-1</sup> ) (s.d.)	114.0 (33.4)	114.0 (34.7)	NS
Mean blood triglycerides (mg dl <sup>-1</sup> ) (s.d.)	104.9 (59.6)	105.3 (58.0)	NS
Median Shannon diversity [IQR]	4.34 [4.04-4.60]	4.31 [3.99-4.57]	0.032
Median Observed OTUs [IQR]	276 [217-247]	287.5 [226-371]	4.60E-05
Mean Bray-Curtis uniqueness (s.d.)	0.24 (0.06)	0.26 (0.07)	3.94E-08

706  
707  
708  
709  
710  
711  
712  
713  
714  
715  
716  
717

**Table S1. Arivale cohort characteristics stratified by microbiome vendor**

Statistical tests used to compare groups are as follows: independent samples t-tests were used for comparing age, body mass index (BMI), high density lipoprotein (HDL), low density lipoprotein (LDL), blood triglycerides and Bray-Curtis Uniqueness; nonparametric Mann-Whitney U tests were used to compare Shannon diversity and Observed OTUs;  $\chi^2$  tests were used to compare sex (percentage female) and race (percentage non-white). *P*-Values  $<0.05$  are colored in red.

718  
719  
720  
721  
722  
723  
724  
725  
726  
727  
728  
729  
730  
731  
732  
733  
734  
735  
736  
737

	<b>Composite Healthy (n=133)</b>	<b>Rest of Cohort (n=466)</b>	<b>Whole Cohort (N=599)</b>	<b>P-Value</b>
Median age (s.d.))	83.5 (3.6)	84.4 (4.2)	84.2 (4.1)	<b>0.013</b>
Mean BMI (s.d.)	26.6 (3.6)	27.1 (3.8)	27.0 (3.8)	0.17
Hispanic (%)	3.8	1.5	2.0	0.15
Mean Shannon diversity (s.d.)	3.6 (0.6)	3.5 (0.6)	3.5 (0.6)	0.58
Mean Observed Species (s.d)	161.0 (50.7)	155.6 (53.1)	156.8 (52.5)	0.29
Diabetes (%)	6.0	17.8	15.2	<b>0.001</b>
Congestive heart failure (%)	0.0	10.5	8.2	<b>&lt;0.001</b>
Hypertension/high blood pressure (%)	41.4	56.7	53.3	<b>0.003</b>
COPD (%)	6.0	12.0	10.7	0.069
Depression (%)	8.3	9.9	9.5	0.70

738  
739 **Table S2. MrOS discovery cohort characteristics stratified into composite healthy and  
remainder of cohort**

740 Statistical tests used to compare groups are as follows: independent samples t-tests were used for  
741 comparing age, body mass index (BMI), Shannon diversity and Observed Species;  $\chi^2$  or Fisher's  
742 exact (if assumptions of  $\chi^2$  were not met) tests were used to compare ethnicity (percentage  
743 Hispanic), and prevalence of each of the specified diseases. P-values  $<0.05$  are colored in red.  
744

745  
746  
747

748  
749  
750  
751  
752  
753  
754  
755  
756  
757  
758  
759  
760  
761  
762  
763  
764  
765  
766  
767

Analyte	P-Value	r_squared	B-coefficient	Missing	Age adj. B-coefficient	Age adj. P-Value
Age	<b>5.89E-33</b>	3.85901529	0.00093261	0	NA	NA
Prescription Med	<b>0.00017481</b>	1.53219831	0.01510618	914	0.00341449	0.08545254
HDL	<b>3.03E-08</b>	0.8659935	0.00549509	104	0.003964398	<b>5.47E-05</b>
n6/n3	<b>3.66E-08</b>	0.855769	-0.0054647	104	-0.003148386	<b>0.00156995</b>
Vitamin D	<b>1.08E-07</b>	0.79702949	0.00527528	104	0.003159677	<b>0.00144512</b>
Alcohol	<b>1.36E-05</b>	0.5608151	-0.0070819	3349	-0.002982965	0.0028601
Homocysteine	<b>0.00014395</b>	0.4087152	0.00377064	104	0.001589201	0.10941824
BMI	<b>0.00044766</b>	0.36457364	-0.0005975	260	-0.003869322	<b>0.00010072</b>
Triglycerides	<b>0.00077075</b>	0.32005925	-0.0033549	104	-0.004164096	<b>1.97E-05</b>
Diarrhea	0.00238587	0.26867461	-0.0040083	3415	-0.001701617	0.08690565
HbA1c	0.00715616	0.204807	0.00272545	104	6.97E-05	0.94455438
Race(ref.white)	0.01700183	0.16061072	0.0058388	88	0.000687553	0.48477659
Antibiotics	0.05402505	0.14773123	0.00642737	2500	0.001844306	0.10335017
Sex	0.02355609	0.14101656	0.00452064	0	0.00236889	0.01379305
Sweets	0.27161453	0.13414917	-0.0012896	902	-4.21E-05	0.98258201
ALAT	0.04087102	0.11844347	-0.0020499	104	-0.002165898	0.02620547
CRP	0.04604621	0.11274027	-0.0019787	104	-0.001966477	0.04354322
LDL	0.04967172	0.10913342	-0.0019505	104	-0.003130326	<b>0.00137829</b>
Glucose	0.10416215	0.07481646	0.00163161	104	-0.000440919	0.6562693
Tobacco	0.11771405	0.07460265	-0.0077207	3264	-0.00115745	0.2504751
Globulin	0.13060992	0.06475052	-0.0015033	104	-0.000324745	0.74022842
ALP	0.18418122	0.0499728	0.00133152	104	-0.000589978	0.55024706
GGT	0.25345563	0.03695739	-0.0011321	104	-0.0023493	0.01643053
Grains	0.32021289	0.029105	-0.0012634	3379	-0.000165682	0.86721005

Fruits	0.34161948	0.02630667	0.00113363	3422	-0.000172467	0.86142995
Insulin	0.48819587	0.0136181	-0.0006939	104	-0.001210903	0.21445978
Vegetables	0.84610634	0.0010959	0.00022377	3422	-0.000193127	0.84450268
Sodium	0.89643796	0.0004802	0.00012949	104	-0.000934367	0.33958969
Sleep	0.93138998	0.000316	0.00021369	2335	0.000427359	0.71350207
HOMA-IR	0.95318368	9.77E-05	-5.85E-05	104	-0.000840639	0.38949581
Creatinine	0.98900622	5.38E-06	-1.37E-05	104	-0.000570523	0.55888158

768      **Table S3. Associations between Bray-Curtis gut microbiome uniqueness and clinical,**  
769      **demographic, and diet/lifestyle/health measures.** ‘P-Value’ corresponds to the unadjusted P-  
770      Value of the  $\beta$ -coefficient (B-Coefficient column) for each analyte from an OLS model adjusted  
771      for gut microbiome vendor. ‘r\_squared’ reflects the percent of variance explained beyond  
772      microbiome vendor for each analyte independently. ‘Missing’ shows the number of missing  
773      observations for each analyte. ‘Age adj. B-coefficient’ and ‘Age adj. P-value’ correspond to the  
774       $\beta$ -coefficient and P-Value for each analyte adjusting for gut microbiome vendor and age. Values  
775      highlighted in red are statistically significant after multiple-hypothesis correction (Bonferroni P-  
776      Value<0.05).

777

778

779

780

781

782

783

784

785

786

787

788

789

790

791

792

793

794

795

796

797

798

799

800

801

Metabolite	P-Value	Corrected P-Value	Adj. B-coefficient
phenylacetylglutamine	3.65E-20	2.38E-17	0.015774767
p-cresol glucuronide*	6.76E-13	4.40E-10	0.011978401
6-hydroxyindole sulfate	7.06E-09	4.60E-06	0.009597508
3-indoxyl sulfate	5.24E-07	0.00034152	0.008269926
lithocholate sulfate	7.39E-07	0.00048191	0.008153816
p-cresol sulfate	5.06E-06	0.00329597	0.007949108
indoleacetate	9.55E-06	0.00622582	0.007363627
taurolithocholate 3-sulfate	6.67E-05	0.04347711	0.006750892
trimethylamine N-oxide	8.02E-05	0.0522833	0.006676801
glycodeoxycholate 3-sulfate	0.00011043	0.07199921	0.006384711
1,5-anhydroglucitol (1,5-AG)	0.00019356	0.12620424	-0.006192382
biliverdin	0.00026726	0.17425604	-0.006295182
carotene diol (1)	0.00048694	0.3174862	-0.006178362
4-ethylcatechol sulfate	0.00059272	0.38645107	0.005838135
threonate	0.00095377	0.6218559	-0.005560642
dodecanedioate (C12-DC)	0.00121002	0.78893024	0.005391288
N-acetylputrescine	0.00448236	1	0.004753617
carotene diol (3)	0.00272636	1	-0.005152625
ergothioneine	0.00708238	1	-0.004510327
androstenediol (3alpha, 17alpha) monosulfate (2)	0.00935419	1	-0.004964594
3-hydroxy-2-ethylpropionate	0.00904741	1	0.004420961
4-ethylphenylsulfate	0.00586104	1	0.004664238
propionylglycine	0.00191267	1	0.005169723
isobutyrylcarnitine (C4)	0.00383686	1	0.004969195
tartronate (hydroxymalonate)	0.00388	1	-0.004950944
cys-gly, oxidized	0.00874903	1	0.004322096
4-acetamidobutanoate	0.0028892	1	0.00512429
bilirubin (Z,Z)	0.00233088	1	-0.005203709
cortisol	0.00512227	1	0.004670237
5-methylthioadenosine (MTA)	0.00432121	1	0.00487853
androstenediol (3beta,17beta) disulfate (2)	0.0078715	1	-0.005096967
2,3-dihydroxy-5-methylthio-4-pentenoate (DMTPA)*	0.00233228	1	0.005882396

802

803

**Table S4 Associations between Bray-Curtis gut microbiome uniqueness and plasma metabolites.** Only metabolites with P-value<0.01 are shown. ‘P-Value’ corresponds to the

804 covariate adjusted P-value of the  $\beta$ -coefficient (Adj. B-coefficient). ‘Corrected P-Value’  
805 corresponds to the Bonferroni corrected P-values. Metabolites significantly associated with  
806 Bray-Curtis uniqueness after adjusting for covariates and multiple hypothesis correction are  
807 highlighted in red. \* indicates metabolites that were confidently identified on the basis of mass  
808 spectrometry data, but for which no reference standards are available to verify the identity.

809  
810  
811  
812

	>8 Meds (N=307)	$\leq$ 8 Meds (N=292)	P-Value
Median age (s.d.)	84.1 (4.0)	84.4 (4.2)	0.33
Mean BMI (s.d.)	27.4 (3.9)	26.6 (3.7)	0.015
Hispanic (%)	2.0	2.1	0.84
Mean Shannon diversity (s.d.)	3.5 (0.6)	3.6 (0.6)	0.021
Mean Observed Species (s.d.)	150.4 (50.8)	163.5 (53.6)	0.002
Diabetes (%)	21.5	8.6	<0.001
Congestive heart failure (%)	13.4	2.7	<0.001
Hypertension/high blood pressure (%)	62.5	43.5	<0.001
COPD (%)	16.6	4.5	<0.001
Depression (%)	11.1	7.9	0.23

813 **Table S5. MrOS discovery cohort characteristics stratified by medication use**

814 Statistical tests used to compare groups are as follows: independent samples t-tests were used for  
815 comparing age, body mass index (BMI), Shannon diversity and Observed species;  $\chi^2$  or Fisher’s  
816 exact (if assumptions of  $\chi^2$  were not met) tests were used to compare ethnicity (percentage  
817 hispanic) and prevalence of each of the specified diseases. *P-Values* <0.05 are colored in red.

818  
819  
820  
821  
822  
823  
824  
825  
826  
827  
828  
829  
830  
831  
832  
833  
834  
835

836  
837  
838